EFFECTS OF RARE EARTH ELEMENTS AND CALCIUM UPON HIGH TEMPERATURE OXIDATION OF AUSTENITIC HEAT-RESISTING ALLOY CONTAINING HIGH SILICON

T. FUJIOKA, M. KINUGASA AND S. IIZUMI

NISSHIN STEEL CO., LTD., SHUNAN WORK, JAPAN

Abstract

Recently, austenitic heat-resisting alloy containing high Si has been considered as a material to be used for automobile exhaust-emission-control system, for example the thermal reactor. The authors have studied the effects of rare earth elements and Ca addition upon the oxidation behaviors of 19% Cr-13%Ni-3%Si-Fe system alloy, in order to improve the oxidation resistance of this alloy.

The following results were obtained :
1) The oxidation resistance of the present alloys was markedly improved with the addition of rare earth elements and / or Ca. 2) However, the differences in the effect upon the oxidation behaviors between rare earth elements and Ca addition were recognized. The addition of rare earth elements improved markedly the scaling resistance and the spalling resistance up to 1100 ℃, but did not improved the scaling resistance at 1200 ℃. On the contrary, the addition of Ca improved remarkably the scaling resistance up to 1200 ℃ and the spalling resistance at 1000 ℃, but did not improved the spalling resistance at 1100 ℃ so much, The complex addition of suitable amount of rare earth elements and Ca was very effective for both the scaling resistance and the spalling resistance up to high temperature. 3) It appears that the good scaling resistance up to high temperature is kept by the protective surface oxide which consists of Cr_2O_3 and spinel type oxide such as $MnO \cdot Cr_2O_3$, and the uniform layer of SiO_2 at the interface of surface oxide and metal because they act as barriers against the diffusion of cations. The good spalling resistance is due to the thin protective surface oxide and the internal oxide consisting of SiO_2 which is formed at the interface of surface oxide and metal under cyclic heating, as if rooting deeply in matrix. This internal oxide, which probably plays a role as a binder of surface oxide and matrix, is promoted with increasing of rare earth elements. However, any accumulation of rare earth elements and Ca, or their oxides have been not detected anywhere.

Introduction

For heat-resisting alloys to be used in automotive exhaust-emission-control devices, such as a thermal reactor, adequate high-temperature strength and oxidation resistance are mainly required. Recently, austenitic heat-resisting alloy containing high Si, such as 19%Cr-13%Ni-3%Si-Fe system alloy, has been considered as a material for these devices because of its adequate high-temperature strength, oxidation resistance and low price. The thermal reactor is classified to two kinds which are the lean thermal reactor and the rich thermal reactor. The lean thermal reactor utilizes a lean fuel-air mixture, consequently operation temperature are lower than those of the rich thermal reactor. The rich thermal reactor is relatively high in hydro-carbon and carbon-monoxide content of its exhaust gas, so that excess of air is used for the oxidation of hydro-carbon and carbon-monoxide. Maximum temperature of exhaust gas in the latter reactor have attained to about 1100 °C. Abnormal operating conditions, such as misfiring, can result in temperatures of 1200 °C and above. Thus, generally speaking, the high-temperature strength and oxidation resistance which correspond to Type 310S are required at least. The 19%Cr-13%Ni-3%Si-Fe system alloy is very economical compared with Type 310S, while its high-temperature oxidation resistance is not always adequate at high temperature. Therefore, in order to improve the oxidation resistance of this alloy, the authors have studied the effects of rare earth elements and Ca additions upon its oxidation behaviors, such as isothermal and cyclic oxidation in air at 1000 °C to 1200 °C. These rare earth elements have been used to improve the oxidation resistance of heat-resisting alloys in the past,[1)~5)] while Ca has almost never been used.

Experimental procedures

Materials

The materials used in the present study are listed in Table 1 with their chemical composition. Every alloy shown in Table 1, except Type 310S which was comercially produced, were melted in high frequency in air and cast into 30kg ingots. Rare earth elements were added by La and Ce rich metal (total rare earth elements:97%), and Ca was added by Ca-Si alloy after the deoxidation by Al. These ingots were subsequently forged to plates (10 x 110 x 500 mm), and thin plates were produced by the following procedure.

1) The hot plates were heated at 1100 °C for 1 hours and then planed to more thin plates (5.0 x 100 x 500 mm) by shaper.
2) These plates were given 60% reduction by cold rolling, and then heat-treated at 1100 °C for a few minutes to make grain size into ASTM NO. 7.0 - 8.0 and air-cooled.

Table 1 Chemical compositions of specimens (Wt %)

No.	chemical compositions						
	C	Si	Mn	Ni	Cr	T·REM*	Ca
S 2	0.05	3.11	0.82	12.88	18.13	—	—
R 1	0.06	3.23	0.66	12.94	18.07	0.094	—
R 2	0.07	3.40	0.85	13.16	17.98	0.009	—
R 3	0.07	3.30	0.80	13.41	18.11	0.020	—
R 4	0.05	3.11	0.68	12.93	17.98	0.184	—
RC 1	0.06	3.93	0.83	13.27	18.01	0.014	0.0039
RC 2	0.05	4.08	0.85	13.15	19.32	0.035	0.0096
RC 3	0.06	3.13	0.68	13.11	18.19	0.203	0.0077
RC 4	0.07	2.18	0.88	13.05	21.05	0.029	0.0073
C 1	0.06	3.71	0.78	13.27	18.54	—	0.0076
C 2	0.07	3.59	0.77	13.02	18.27	—	0.0029
C 3	0.07	3.55	0.83	13.00	18.39	—	0.0220
Type 310S	0.07	0.79	1.58	19.50	24.85	—	—

* Total amount of rare earth elements

Isothermal oxidation test

Prior to testing, the specimens (2.0 x 25 x 35 mm) were polished with 400 grit emery paper, measured with a micrometer to the nearest 0.001 mm, and degreased with acetone. After weighing to the nearest 1.0mg, these specimens were respectively placed into alumina crucibles to retain no-adherent oxide scale, and then oxidized in air in laboratory muffle-type furnace at 1000° to 1200 °C up to 215 hours. After isothermal oxidation test, each alumina crucible was immediately covered to prevent scattering away of the oxide scale and gradually cooled, and then the specimens and spalled oxide scales were weighed together to the nearest 1.0 mg.

Moreover, in some alloys, isothermal oxidation tests at 1200 °C were conducted by thermal balance. The used specimens (2.0 x 15 x 25 mm) were prepared by the above similar menthod. The weight change in this test was recorded continuously, and measured to the nearest 0.5 mg.

Cyclic oxidation test

These test specimens (2.0 x 30 x 50 mm) were also prepared by the method similar to the above. After weighing to the nearest 1.0 mg, the specimens were respectively suspended in a vertical furnace The specimens were automatically raised and lowered between room temperature and high temperature.
This test was carried out at 1000° and 1100 °C, and the heat cycle consisted of heating at the testing temperature for 25 minutes and cooling at room temperature for 5 minutes. The weight changes were measured every 50 cycles after removing the loose oxide. So, the spalled oxide was not included in the weight of the specimens in this test.

X-ray diffraction, electron probe micro-analysis, and metallographic examination

After each oxidation test, the structure of oxide layers and the distribution of alloying elements in the oxide layers and substrata have been investigated by X-ray diffraction and the electron probe micro-analysis techniques in order to clarify the mechanism of the effect of rare earth elements (hereafter written as REM) and Ca additions upon the oxidation behaviors of the present alloys. Metallographic examinations were carried out prior to electron probe micro-analysis. The transverse sections of the specimens were investigated for the electron probe micro-analysis and metallographic examination in non-etched state.

Results and Discussion

Isothermal oxidation

Usually, it is assumed that an oxidation process of alloy follows the parabolic rate law as shown following equation

$$\Delta W = kp.t^{1/2}$$

where ΔW is the specific weight changes; t, heating time ; kp, isothermal oxidation rate constant. Therefore a plot of specific weight gain (mg/cm^2) against time ($hr^{1/2}$) was also used in this study. The results are shown in Fig. 1. These data indicated that the isothermal oxidation process of RC1, C3 and Type 310S alloys approximately followed the parabolic rate law at all temperature, although those oxidation rate were respectively different. On the contrary, the oxidation process of S2, R1 and RC3 alloys followed the parabolic rate law up to 1100 °C, but not at 1200 °C. S2 and RC3 alloys oxidized with shifting from the parabolic rate law in long time test even at 1100 °C.

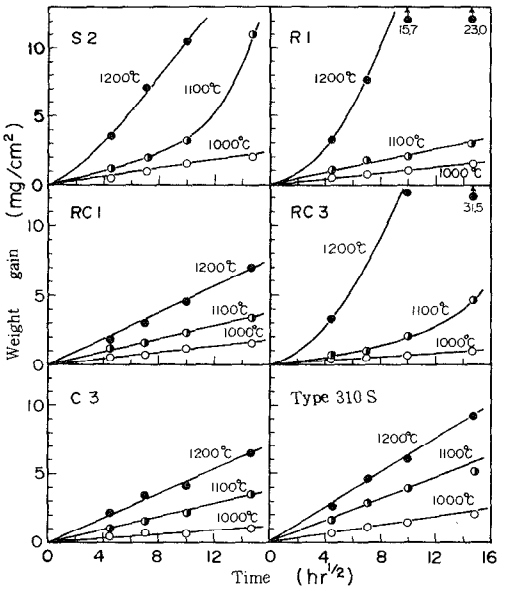

Fig. 1 Parabolic plots of isothermal oxidation data

The isothermal oxidation rate constant kp derived from Fig. 1 are represented in Fig 2 as an Arrhenius plots. The isothermal oxidation rate constant kp of S2 and R1 alloys at 1200 ℃, however, were roughly determined, and the kp of S2 alloy at 1100 ℃ were determined from the relation of ΔW-time in 100 hours. These indicated that the temperature dependence of kp was approximately similar in all alloys within following to the parabolic rate law. Moreover, the oxidation resistance of present alloys was markedly improved by the addition of REM and / or Ca. However, the difference in the effect upon the isothermal oxidation behaviors between REM and Ca addition was recognized. The addition of REM, such as R1 alloy, markedly reduced the isothermal oxidation rate up to 1100 ℃, but did not at 1200 ℃. On the contrary, the addition of Ca, such as C3 alloy, markedly reduced the isothermal oxidation rate up to 1200 ℃ for its content.

The complex addition of REM and Ca, such as RC 1 alloy reduced the isothermal oxidation rate up to 1200 ℃ similar to the addition of Ca, but increased the isothermal oxidation rate above 1100 ℃, when REM content was substantial, such as RC3 alloy. The ΔW-time plots obtained from the thermal balance at 1200 ℃ is represented for S2, R1 and C3 alloys in Fig. 3. This result indicated that R1 alloy oxidized in accordance with the parabolic rate law in initial stage, and the kp of R1 alloy was considerably smaller than that of S2 alloy. However, R1 alloy with REM suddenly oxidized in accordance with the linear rate law after about 15 hours, which was presumably due to the loss of protectivity of surface oxide. On the contrary, the surface oxide formed on C3 alloy with Ca may maintain the protectivity for long time even at 1200 ℃.

The ΔW-time plots for R series containing only REM and C series containing only Ca are represented in Fig. 4 and Fig. 5 respectively. Fig. 4 showed that the isothermal oxidation rate at 1100 ℃ was considerably reduced with increasing the amount of REM up to about 0.1%, while the excess REM addition such as 0.184% increased the isothermal oxidation rate even at 1100 ℃. At 1200 ℃, the isothermal oxidation rate increased remarkably with REM content, moreover, the oxidation process of these alloys was in accordance with the linear rate law, but in the initial stages the isothermal oxidation process of these alloys was in accordance with the parabolic rate law even at 1200 ℃ as mentioned above.

On the other hand, the addition of Ca reduced considerably the isothermal

oxidation rate up to 1200 ℃. The effects of the amount of Ca upon the oxidation rate was not clear in this study as shown in Fig. 5, but it is assumed that the Ca addition more than in this study does not improve the oxidation rate.

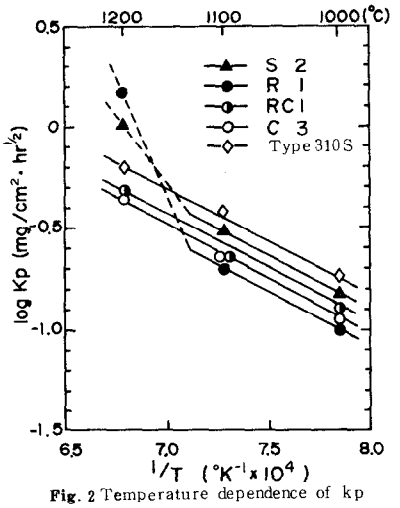

Fig. 2 Temperature dependence of kp

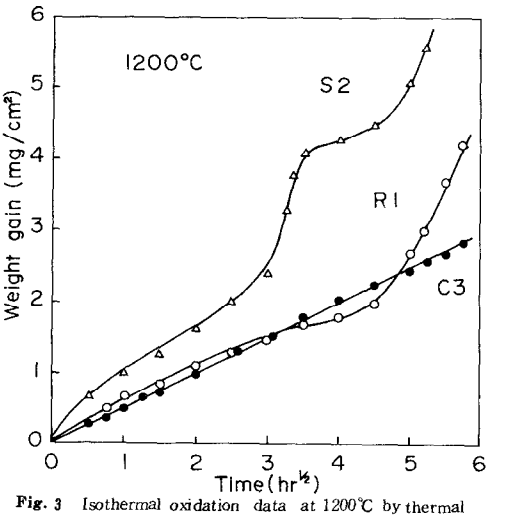

Fig. 3 Isothermal oxidation data at 1200℃ by thermal balance

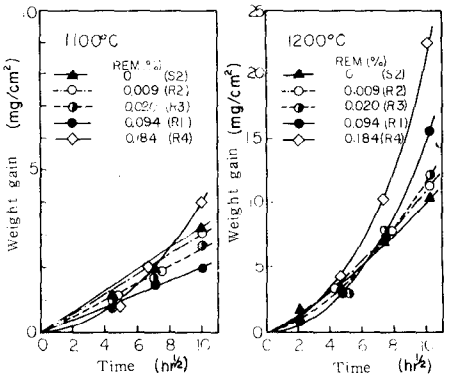

Fig. 4 Effect of REM content upon scaling resistance

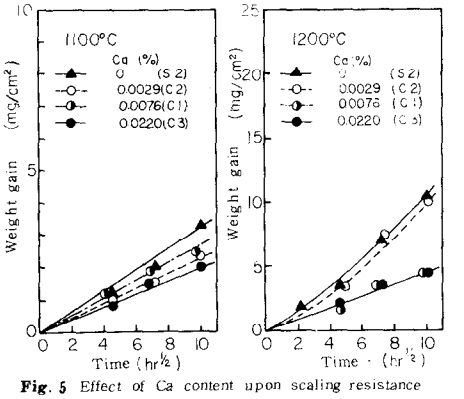

Fig. 5 Effect of Ca content upon scaling resistance

Cyclic oxidation

Weight change against cycles are shown in Fig. 6 (at 1000 ℃) and Fig. 7 (at 1100 ℃). The relations of the total weight loss to the REM and / or Ca content are shown in Fig. 8 (1000 cycles at 1000 ℃) and Fig. 9 (500 cycles at 1100 ℃) respectively. It was deduced from these data that the spalling resistance in the present alloys was improved with the addition of REM and / or Ca, but the different effects in the spalling behaviors between REM and Ca addition was recognized.

The specimens containing only REM such as R1 and R4 alloys in Fig. 6, began to spall in comparatively initial stage at 1000 ℃, but the weight change did not markedly show and resulted in small weight loss during the testing. On the contrary, the specimens containing only Ca such as C1 and C3 alloys in Fig. 6, delayed markedly in the cycle number to begin the spalling for its content, and the total weight loss were reduced to comparatively small quantity. In addition, the specimens containing REM and Ca such as RC1, RC2 and RC3 alloys were very

similar to the specimens containing only Ca in spalling behavior. The total weight loss was reduced with increasing content of REM and Ca. The spalling behaviors at 1100 ℃ about the specimens containing only REM was similar to that at 1000 ℃.

The specimens containing only Ca, such as C3 in Fig. 7, delayed slightly in the cycle number to begin the spalling, while their weight loss was not reduced so much. It is assumed from this fact that the surface oxides formed at 1100 ℃ on the specimens containing only Ca are easy to spall on cooling. However, the complex addition of REM and Ca could improve the weak point, that is to say, the specimens containing REM and Ca, such as RC1, RC2 and RC3 alloys, delayed in the cycle number to begin the spalling and were reduced to a small amount in the total weight loss. In this case, the more the total amount of REM and Ca increased, the more the effect of improvement became remarkable. Therefore, the complex addition of the suitable amount of REM and Ca was very effective for the improvement of spalling resistance in the present alloys up to high temperature.

On the other hand, RC4 alloy containing comparatively small content of Si and much content of Cr was very superior in the spalling resistance, as shown in Fig. 6 and Fig, 7. This fact may suggest that the investigation of the effect of Cr content upon the spalling resistance is very important.

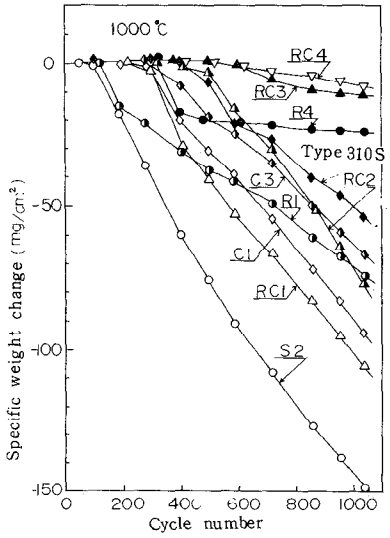

Fig. 6 Specific weight change in cyclic oxidation at 1000 ℃

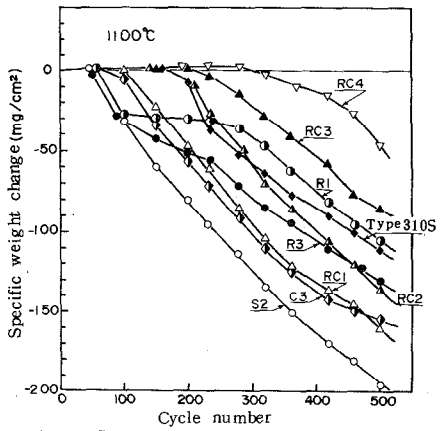

Fig. 7 Specific weight change in cyclic oxidation at 1100 ℃

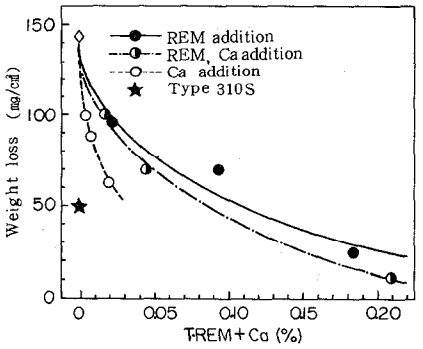

Fig. 8 Effect of REM and Ca content upon spalling resistance at 1000℃ (Weight loss was obtained after cyclic oxidation of 1000 cycles.)

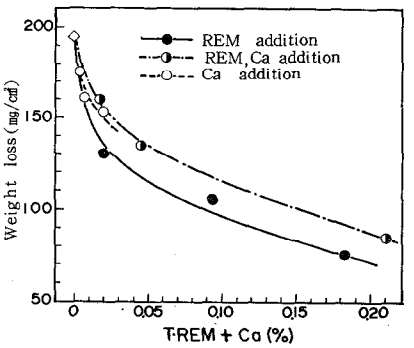

Fig. 9 Effect of REM and Ca content upon spalling resistance at 1100℃ (Weight loss was obtained after cyclic oxidation of 500 cycles.)

Analysis of oxide

The surface oxides which spalled on cooling after isothermal oxidation at each temperature for 50 hours, and the oxide layers which were adhering on the specimens after cyclic oxidation at 1100 °C for 500 cycles were identified with X-ray diffraction method for some specimens. The results obtained are represented in Table 2. All specimens after isothermal oxidation at 1000° and 1100 °C were covered with the surface oxide consisting of Cr_2O_3 and spinel type oxide. S2 alloy was covered with the oxide consisting of $(Fe, Cr)_2O_3$ and spinel type oxide at 1200 °C, while R1, R4, RC3 and Type 310S alloys were covered with the oxide consisting of Cr_2O_3, spinel type oxide and $(Fe,Cr)_2O_3$. RC1, C1 and C3 alloys were covered with the oxide consisting of Cr_2O_3 and spinel type oxide, similar to the oxide formed at 1000 °C and 1100 °C testings. Therefore, this showed that the surface oxides formed on the specimens which oxidized in accordance with the parabolic rate law consisted of Cr_2O_3 and spinel type oxide with the exception of Type 310S, but the surface oxide formed on the specimens which oxidized with shifting from the parabolic rate law consisted of $(Fe, Cr)_2O_3$ and spinel type oxide, or Cr_2O_3, spinel type oxide and $(Fe, Cr)_2O_3$.

Table 2 X-ray diffraction results

	1000℃ ×50hr	1100℃ ×50hr	1200℃ ×50hr	1100℃ 500cycles
S 2	Cr_2O_3 SP.	Cr_2O_3 SP.	$(Fe,Cr)_2O_3$ SP.	SP. $(Fe,Cr)_2O_3$
R 1	Cr_2O_3 SP.	Cr_2O_3 SP.	Cr_2O_3, SP. $(Fe,Cr)_2O_3$	SP. $(Fe,Cr)_2O_3$
R 4	Cr_2O_3 SP.	Cr_2O_3 SP.	Cr_2O_3, SP. $(Fe,Cr)_2O_3$	SP. $(Fe,Cr)_2O_3$
RC 1	Cr_2O_3 SP.	Cr_2O_3 SP.	Cr_2O_3 SP.	SP. $(Fe,Cr)_2O_3$
RC 3	Cr_2O_3 SP.	Cr_2O_3 SP.	Cr_2O_3, SP. $(Fe,Cr)_2O_3$	SP. $(Fe,Cr)_2O_3$
C 1	Cr_2O_3 SP.	Cr_2O_3 SP.	Cr_2O_3 SP.	SP. $(Fe,Cr)_2O_3$
C 3	Cr_2O_3 SP.	Cr_2O_3 SP.	Cr_2O_3 SP.	SP. $(Fe,Cr)_2O_3$
Type 310S	Cr_2O_3 SP.	Cr_2O_3 SP.	Cr_2O_3, SP. $(Fe,Cr)_2O_3$	SP. $(Fe,Cr)_2O_3$

SP : Spinel type oxide

On the other hand, the oxide adhering on the specimens after cyclic oxidation consisted of spinel type oxide and Cr_2O_3 in all specimens. However, the particular oxide of REM or Ca, and alpha-cristobarite were not detected in all cases. Then the distribution of main metal elements and oxygen from oxide layer to substratum was observed by electron probe micro-analyser for some specimens after isothermal oxidation at 1200 °C for 50 hours and cyclic oxidation at 1100 °C for 500 cycles. Photo 1 and Photo 2 showed these results. The results of observation showed that Fe and Ni were detected, but not Cr in the surface oxide adhering on S2 and R1 alloys, which were inferior in the isothermal oxidation resistance at 1200 °C as shown in Photo. 1. The Cr depleted zone was widely taken in those substrata. However there were differences in Cr concentration of surface oxide and a form of the internal oxide layers consisting of SiO_2 between S2 and R1 alloys. That is to say, the surface oxide of S2 alloy contained Fe and Ni more than that of R1 alloy, and uniform internal oxide layers consisting of SiO_2 were clearly separated from the surface oxide, while the adhering surface oxide of R1 alloy consisted of Cr rich oxide with Mn distributed uniformly, and the internal oxide layer formed in R1 alloy mixed with the surface oxide. In addition, the internal oxide consisting of SiO_2 were rooted deeply into matrix. Fe and Ni were not almost detected from the surface oxide adhering on RC1 and C1 alloys, and this may be due to their good scaling resistance. The surface oxide formed on RC1 and C1 alloys consisted of Cr rich oxide containing Mn, so that those oxides may be Cr_2O_3 and $MnO \cdot Cr_2O_3$.

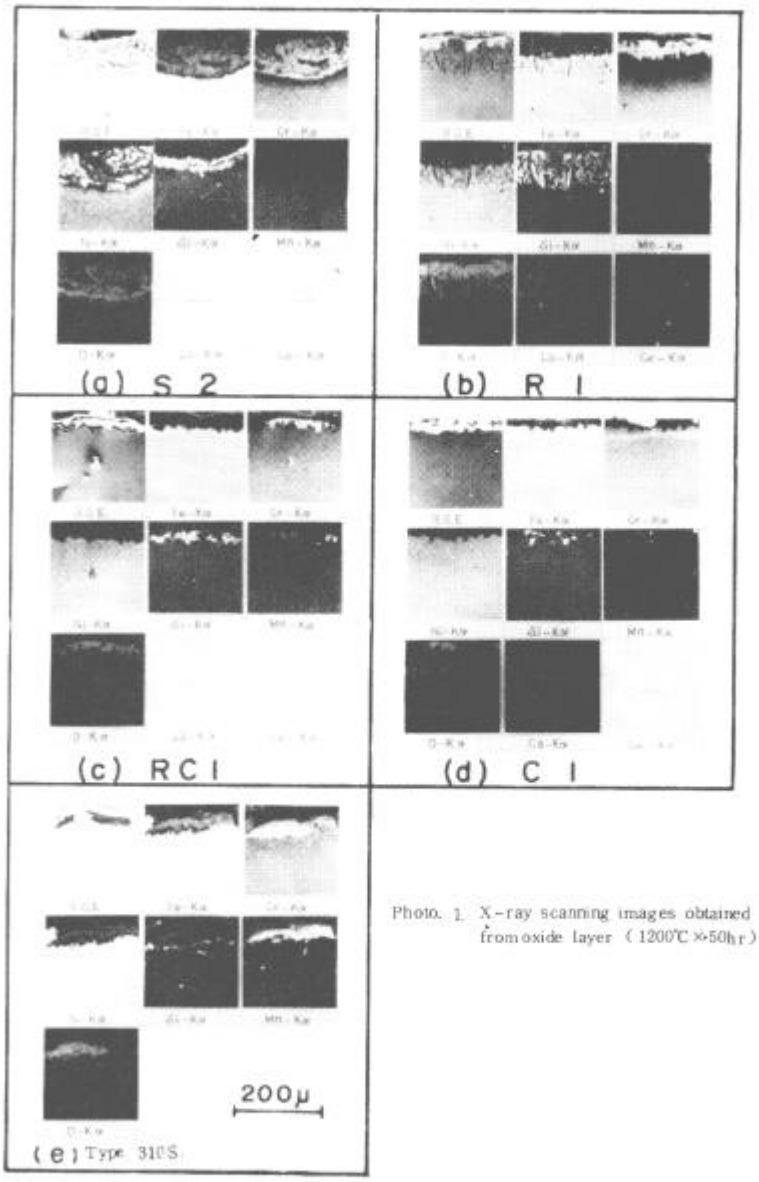

Photo. 1 X-ray scanning images obtained from oxide layer (1200℃×50hr)

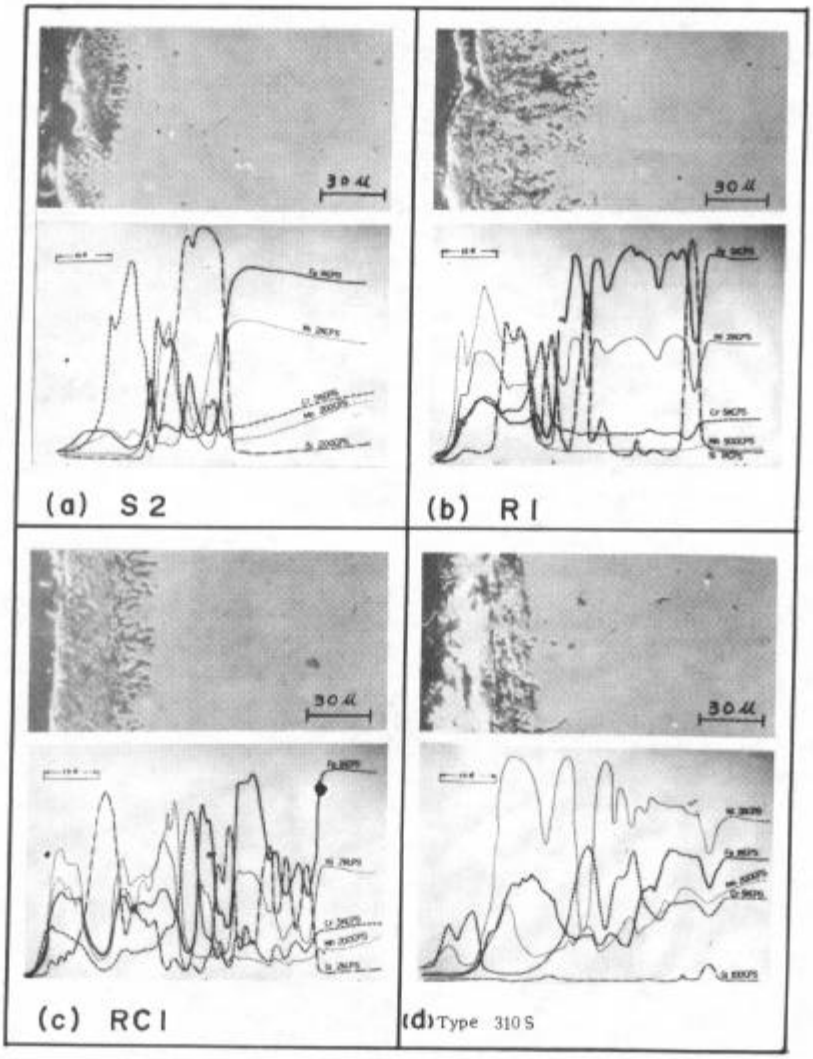

Photo. 2. Distribution of some elements from oxide layers to substrata by scanning electron probe micro-analysis (1100℃, 500 cycles)

The internal oxide formed in RCl alloy containing both REM and Ca mixed with the surface oxide and was rooted in matrix, although the internal oxide was not formed deeply as that of Rl alloy. However, such a fact was not clearly obserbed from that of Cl alloy containing only Ca, because the surface oxide was very easy to spall on cooling after oxidation test. All specimens after cyclic oxidation were covered with the surface oxide which contained much quanity of Ni and Fe as shown in photo 2, and the internal oxide consisting of SiO_2 formed beneath the surface oxide. The surface oxide adhering on Rl and RCl alloys which were comparatively superior in the spalling resistance, contained much Mn, and the internal oxide of the both alloys rooted deeply in matrix in comparison with the others. This fact was considerably recognized about Rl alloy containing much REM. It was deduced from these results that the good scaling resistance up to high temperature in the present alloys was kept by the protective surface oxide which consisted of Cr_2O_3 and spinel type oxide such as $MnO \cdot Cr_2O_3$, and a uniform SiO_2 layer playing a role as the barrier against the diffusion of cations at the interface of surface oxide and metal. Then it is assumed that the addition of Ca improves remarkably the protectivity of surface oxide up to 1200 °C, and sufficiently lowers the partial oxygen pressure Po_2 beneath surface oxide, so that the uniform and thin SiO_2 layer is formed. As the surface oxide formed on the specimens containing only REM can not maintain the protectivity at 1200 °C, the partial oxygen pressure Po_2 at 1200 °C beneath surface oxide may not be low enough so that the preferential oxidation of Cr and the formation of nonuniform SiO_2 layer are considerably promoted. The Cr depleted zone formed by the preferential oxidation of Cr was accompanied with considerable oxidation, such as Rl alloy at 1200 °C.
The role of Ca in the complex addition of REM and Ca may help the above weak points of REM addition. However, this effect of Ca addition was not obtained in the alloy such as RC3 containing too much REM.

On the other hand, the good spalling resistance in the present alloys may be due to the thin protective surface oxide and the SiO_2 layer which mixes with surface oxide and roots deeply in matrix. This type internal oxide may reduce the thermal stress acting between surface oxide and matrix as compared with the uniform internal SiO_2 layer, and play a role as binder between surface oxide and matrix. The addition of Ca may suppress the growth of surface oxide, so that the start of spalling is delayed. However, as the surface oxide thickens it may become easy to spall, because the internal SiO_2 layer is produced in the metal-surface oxide interface, moreover, it is comparatively uniform. The addition of REM may promote the growth of surface oxide, so that the spalling of oxide occure in the initial stage. After the spalling, however, the formation of comparatively protective surface oxide and SiO_2 layer rooting deeply in matrix is promoted, so that the surface oxide becomes difficult to spall. In the complex addition of REM and Ca, the spalling resistance is improved further with increasing of REM.

From the above, the mechanism that REM and Ca improve the oxidation resistance of the present alloys, is not clear. Probably, those elements may improve the oxidation resistance through some indirect effects.[6),7)]

Summary

The isothermal and cyclic oxidation behavior of 19%Cr-13%Ni-3%Si-Fe system alloys containing small amount of REM and / or Ca was studied in air at 1000° to 1200 °C. The salient results can be summarized as follows:

1. The oxidation resistance of present alloys was markedly improved with the addition of REM and / or Ca.
2. However, the differences in the effect upon the oxidation behaviors between REM and Ca addition were recognized. That is to say, the addition of REM improved markedly the scaling resistance and the spalling resistance up to 1100 °C, but did not improved the scaling resistance at 1200 °C. On the contrary, the addition of Ca improved markedly the scaling resistance up to 1200 °C, and the spalling resistance at 1000 °C, but did not improve the spalling resistance at 1100 °C so much. The complex addition of suitable amount of REM and Ca was very effective for both scaling resistance and spalling resistance up to high temperature.
3. It appears that the good scaling resistance up to high temperature is kept by the protective surface oxide which consists of Cr_2O_3 and spinel type oxide such as $MnO \cdot Cr_2O_3$, and the uniform SiO_2 layer playing a role as the barrier to the diffusion of cations. On the contrary, the good spalling resistance is due to the thin protective surface oxide and the internal oxide consisting of SiO_2, which is formed at the interface of surface oxide and metal under cyclic heating, as if rooting deeply in matrix. This internal oxide which probably plays a role as binder of surface oxide and matrix is promoted with increasing of REM. However, any accumulation of REM and Ca, or their oxides have been not detected anywhere.

References

1) E. J. Felten: J. Electrochem. Soc., 108(1961), 490.

2) Y. Fukase, T. Nishima, K. Osozawa and R. Nemoto: J. Japan Inst. Metals (in Japanese), 32(1968),33.

3) Y. Fukase, K. Osozawa and R. Nemoto: ibid, 33(1969),40

4) Y. Fukase, K. Osozawa and R. Nemoto: ibid, 33(1969),46

5) S. Yajima, Y. Saito and T. Amano : Denkiseiko (In Japanese), 45(1974), 144

6) T. Nakayama and Y. Watanabe: J. Japan Inst. Metals (in Japanese), 31(1967), 4

7) L. Horn: Z. Metallk., 40(1949), 73